UCRL-PROC-234041

Searching for plasmas with anomalous dispersion in the soft X-ray regime

Joseph Nilsen, Walter R. Johnson, K. T. Cheng

August 27, 2007

Disclaimer

This document was prepared as an account of work sponsored by an agency of the United States Government. Neither the United States Government nor the University of California nor any of their employees, makes any warranty, express or implied, or assumes any legal liability or responsibility for the accuracy, completeness, or usefulness of any information, apparatus, product, or process disclosed, or represents that its use would not infringe privately owned rights. Reference herein to any specific commercial product, process, or service by trade name, trademark, manufacturer, or otherwise, does not necessarily constitute or imply its endorsement, recommendation, or favoring by the United States Government or the University of California. The views and opinions of authors expressed herein do not necessarily state or reflect those of the United States Government or the University of California, and shall not be used for advertising or product endorsement purposes.

Searching for plasmas with anomalous dispersion in the soft X-ray regime

Joseph Nilsen[1], Walter R. Johnson[2], and K. T. Cheng[1]

[1]Lawrence Livermore National Laboratory, Livermore, CA 94551
[2]University of Notre Dame, Notre Dame, IN 46556

ABSTRACT

Over the last decade the electron density of plasmas has been measured using X-ray laser interferometers in the 14 to 47 nm wavelength regime. With the same formula used in decades of experiments with optical interferometers, the data analysis assumes the index of refraction is due only to the free electrons, which makes the index less than one. Over the last several years, interferometer experiments in C, Al, Ag, and Sn plasmas have observed plasmas with index of refraction greater than one at 14 or 47 nm and demonstrated unequivocally that the usual formula for calculating the index of refraction is not always valid as the contribution from bound electrons can dominate the free electrons in certain cases. In this paper we search for other materials with strong anomalous dispersion that could be used in X-ray laser interferometer experiments to help understand this phenomena. An average atom code is used to calculate the plasma properties. This paper discusses the calculations of anomalous dispersion in Ne and Na plasmas near 47 nm and Xe plasmas near 14 nm. With the advent of the FLASH X-ray free electron laser in Germany and the LCLS X-FEL coming online at Stanford in 2 years the average atom code will be an invaluable tool to explore plasmas at higher X-ray energy to identify potential experiments for the future. During the next decade X-ray free electron lasers and other X-ray sources will be used to probe a wider variety of plasmas at higher densities and shorter wavelengths so understanding the index of refraction in plasmas will be even more essential.

Keywords: X-ray laser, Interferometers; Index of refraction; Plasmas; Anomalous dispersion

1. INTRODUCTION

From the earliest days of lasers, optical interferometers have been used to measure the electron density of plasmas [1] assuming that the index of refraction of the plasma is due only to the free electrons [1-2]. This assumption makes the electron density of the plasma directly proportional to the number of fringe shifts in the interferometer and further assumes that that the index of refraction in the plasma is always less than one. A decade ago the first X-ray laser interferometer [3] operating at a wavelength of 15.5 nm was demonstrated at the Nova facility at Lawrence Livermore National Laboratory (LLNL). Over the past decade many X-ray laser interferometers [4-6], as well as a high order harmonic interferometer [7], have been built in the wavelength range of 14 to 72 nm. All the data analysis done with these sources assume only the free electrons contribute to the index of refraction. In the future, interferometers will be built using the VUV and X-ray free electron lasers, which will extend lasers to even shorter wavelengths [8].

In the last several years interferometer experiments of Al plasmas [4,5,9], Sn and Ag plasmas [10], and C plasmas [11] have observed fringe lines bend in the opposite direction than was expected, indicating that the index of refraction was greater than one. The traditional analysis of the experiments would indicate that the electron density was less than zero. The original experiments in the Al plasmas were done at the Advanced Photon Research Center at JAERI using the 13.9 nm Ni-like Ag laser [4] and at the COMET laser facility at LLNL using the 14.7 nm Ni-like Pd laser [5]. The analysis of all these experiments show that the anomalous dispersion from the resonance lines and absorption edges of the bound electrons have a large contribution to the index of refraction with the opposite sign as the free electrons and this explains how the index of refraction is greater than one in these plasmas [10-14]. Initially, a surprising result of the calculations is that the influence of the bound electrons on the index of refraction extends far from the absorption edges and resonance lines [12]. Resonance lines affect the index of refraction at photon energies located orders of magnitude further from the line centers than the corresponding line widths owing to the fact that they contribute through a dispersion integral.

The original analysis [12] of the index of refraction for Al plasmas was done at a single wavelength, 14.7 nm, by combining individual calculations done for each iso-electronic sequence of Al. That analysis pointed out the need for a new tool that would let us calculate the index of refraction for any plasma at any wavelength. The INFERNO average atom code has been used for many years to calculate the distribution of levels and the absorption coefficient for plasma at a given temperature and density [15]. By modifying this code [16], we are now able to calculate the index of refraction for a wide range of plasma conditions. To validate the average atom code [13] we compared with calculations done with the more detailed OPAL code [17-19].

In this work we search for other materials that can be used to create plasmas with index of refraction greater than one at X-ray laser energies. We discuss how neutral Na vapor and singly-ionized Ne plasma look to be promising candidates to use in interferometer experiments based on the Ne-like Ar X-ray laser at 26.44 eV. For triply-ionized Xe, we present calculations that show that this plasma will have an index of refraction greater than one at the energy of the Pd X-ray laser at 84.46 eV.

2.   ANALYSIS OF INTERFEROMETER EXPERIMENTS

Assuming only free electrons contribute to the index of refraction, the formula for the index of refraction of a plasma is $n = (1 - N_{elec} / N_{crit})^{1/2}$ where N_{elec} is the electron density of the plasma and N_{crit} is the plasma critical density. At wavelength λ, $N_{crit} = \pi / (r_0 \lambda^2)$ where r_0 is the classical electron radius, 2.818×10^{-13} cm [2]. In typical experiments the electron density is much less than the critical density so the formula above can be approximated by $n = 1 - (N_{elec} / 2N_{crit})$. For a plasma that is uniform over length L the number of fringe shifts observed in an interferometer equals $(1 - n) L / \lambda$. For a non-uniform plasma one does a path length integral. The fringe shifts are referenced against a set of reference fringes in the absence of any plasma and the formula assumes that the interferometer is in a vacuum. Using the approximations described above, the number of fringe shifts equals $(N_{elec} \ L) / (2 \ \lambda \ N_{crit})$. When analyzing an experiment one counts how far the fringes have shifted compared with the reference fringes and converts this into electron density. For the 46.9 nm Ar X-ray laser the number of fringe shifts in the interferometer is $(N_{elec} \ L) / (4.75 \times 10^{18}$ cm$^{-2})$ and the critical density is 5.07×10^{23} cm^{-3}.

For a plasma we can define a complex index of refraction $n^* = 1 - \delta - i\beta$. The real part of the index of refraction $n = 1 - \delta$. The imaginary part of the index of refraction is due to absorption. The total absorption coefficient $\alpha = N_{ion} \ \sigma = (4 \ \pi \ \beta) / \ \lambda$ where N_{ion} is the ion density of the plasma and β is the imaginary part of the complex index of refraction n^*. The Henke tables tabulate the dimensional-less optical constants f_2 and f_1 for neutral materials. These are related to δ and β by $\delta = f_1 N_{ion} / (2 N_{crit})$ and $\beta = f_2 \ N_{ion} / (2 \ N_{crit})$ [20]. From the total absorption cross-section σ we determine the

optical constant $f_2 = \sigma / (2 \lambda r_0)$. We then derive the optical constant f_1 as a function of photon energy E using the Kramers-Kronig dispersion relation [21]. This involves taking the principal value of the integral

$$f_1(E) = Z_{nuc} + \frac{2}{\pi} P.V. \int_0^\infty \frac{f_2(\varepsilon) \, \varepsilon \, d\varepsilon}{E^2 - \varepsilon^2}$$

where Z_{nuc} is the atomic number of the element. This means we include the total number of bound and free electrons when calculating the dispersion relation. For example, $Z_{nuc} = 11$ for a Na plasma. For neutral materials the oscillator sum rules insure that f_1 goes to zero at zero energy and Z_{nuc} at infinite energy. For an ionized plasma with average ionization Z^* then $f_1 = Z^*$ at E = 0.

In the absence of any bound electrons f_1 is equivalent to the number of free electrons per ion. This means that we can replace N_{elec} with $f_1 N_{ion}$ in the formula for the number of fringe shifts. The free electron approximation for the index of refraction is true when f_1 is equal to Z^*. The number of fringe shifts observed in the experiment for a real plasma is now equals $(f_1 N_{ion} L) / (2 \lambda N_{crit})$. Taking the ratio of f_1 to Z^* gives the ratio of the measured electron density to the actual electron density. When the ratio is negative, the index of refraction is greater than one and the fringes bend the opposite direction than expected in the interferometer.

3. AVERAGE ATOM CODE

The INFERNO code [15] has been used for many years to calculate the ionization conditions and absorption spectrum of plasmas under a wide variety of conditions. This code uses the average-atom technique. For finite temperatures and densities, the INFERNO code calculates a statistical population for occupation of one-electron Dirac orbitals in the plasma. We use a non-relativistic version of INFERNO in this work to calculate bound and continuum orbitals and the corresponding self-consistent potential. By applying linear response theory we obtain an average-atom version of the Kubo-Greenwood equation [22,23] for the frequency-dependent conductivity of the plasma. The imaginary part of the complex dielectric function is proportional to the conductivity. The real part of the dielectric function can be found from its imaginary part using a Kramers-Kronig [21] dispersion relation. The details of the Kubo-Greenwood formula applied to the average-atom model are described in Ref. 16.

The average-atom results [13] have been validated against calculations done with the OPAL code [17-19]. The OPAL code was developed at the LLNL to compute opacities of low- to mid-Z elements. In the OPAL code the plasma is treated as a mixture of atoms in discrete ionization states, thereby giving a more realistic description of individual lines and absorption edges. However the OPAL calculations can only be done for a limited range of ions.

To do the calculation of the optical properties of various plasmas, we assume the plasmas have a constant ion density of 10^{20} cm^{-3} and we vary the temperature to change the ionization state of the plasma. Since the average atom code was developed to calculate higher density materials near solid density it is presently difficult to calculate at lower densities than 10^{20} cm^{-3}. In most laser plasmas we are typically dealing with plasmas at this density or one to two orders of magnitude lower density. Even though the calculations are done for a single ion density the optical constants f_1 and f_2 that we calculate normalize away the actual density so we expect the analysis to be valid over a wide range of densities. The code assume the electron, ion, and radiation temperatures are equal and the plasma is in local thermodynamic equilibrium (LTE). For a dynamic plasma that is not in equilibrium, the ionization condition (Z^*) is a good way to compare plasma rather than the actual temperature of the plasma. $Z^* = 1$ means the average ion is singly ionized, 2 means double ionized, etc.
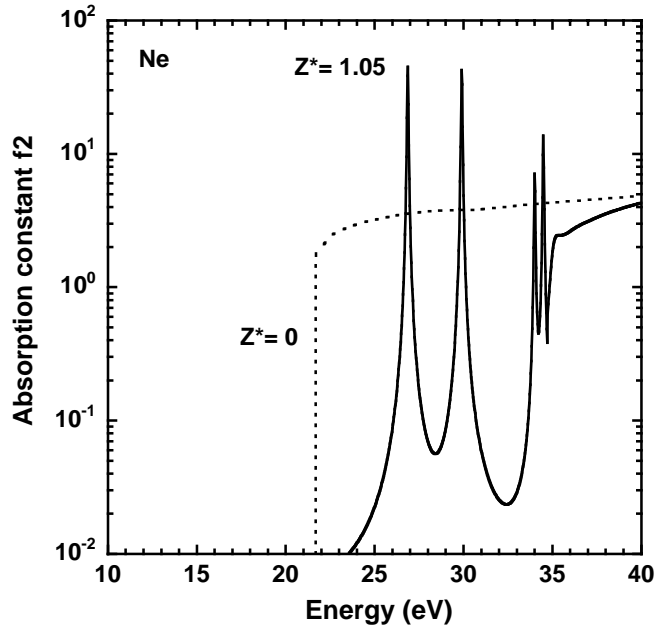
Fig. 1. Absorption constant f_2 versus photon energy for Ne plasmas. The dotted line is from the Henke data. The solid curve is from the average atom code for $Z^* = 1.05$. The average ionization state is given by Z^*. The ion density is 10^{20} cm^{-3}.
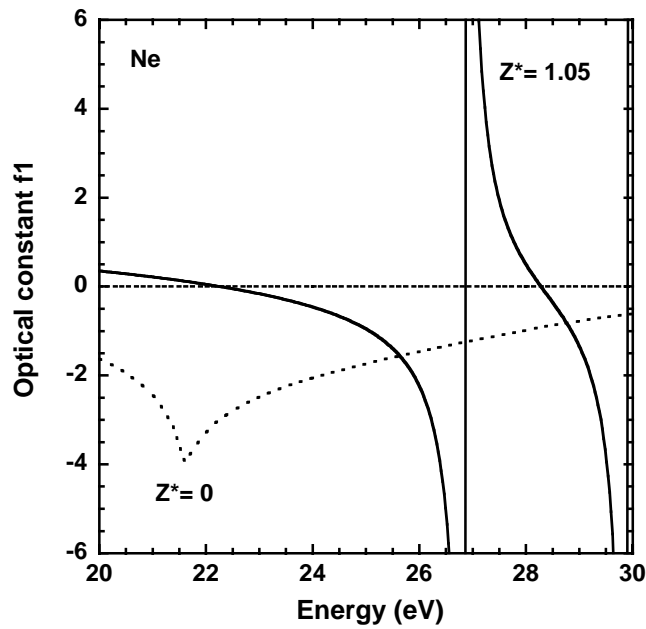

Fig. 2. Optical constant f_1 versus photon energy for Ne plasmas. The dotted line is from the Henke data. The solid curve is from the average atom code for $Z^* = 1.05$. The average ionization state is given by Z^*. The ion density is 10^{20} cm^{-3}. The other dotted line at a value of 0 is a visual aid.

4. MODELING OF NEON AND SODIUM PLASMAS AT 46.9 NM

We have been looking for other plasmas in which we could observe a strong contribution from bound electrons that would make the index of refraction larger than one. For the interferometer that uses the Ne-like Ar X-ray laser at 46.9 nm (26.44 eV) we first looked at the Henke data to find materials with absorption edges in the 20 – 30 eV range. Since Ne and Na both looked like interesting materials with L shell edges at 21.6 and 30.6 eV, respectively, we extrapolated the Henke data to estimate the f_1 versus photon energy for neutral Ne and Na. Finding negative f_1 values for neutral materials is usually a good clue to find negative f_1 in plasma that are only a few times ionized.

For neutral Ne the plasma would be very opaque to the 26.44 eV X-rays since they are above the L-shell absorption edge at 21.6 eV. However for single ionized neon the L-edge moves to 41 eV and the plasma becomes much more transparent as shown in Fig. 1 which plots the absorption constant f_2 versus photon energy for Ne plasmas. The case Z* = 0, shown by the dotted line, is the Henke data. Using an ion density of 10^{20} cm^{-3} at a temperature of 4 eV the average atom code calculates a Z* = 1.05, which is close to singly-ionized. This calculated spectrum, shown by the solid line, is shifted by 4.18 eV to higher energy so that the 2s-2p line agrees with the experimentally measured value of 26.86 eV [24]. Figure 2 shows the optical constant f_1 versus photon energy for the Ne plasmas. For the case Z* = 0, shown by the dotted line, the Henke data has been extrapolated to lower energy. At an energy of 26.44 eV f_1 = -1.4 for the neutral Ne but this case would be highly absorbing. For the singly ionized case with Z* = 1.05, shown by the solid line, f_1 is now –4.4 at the photon energy of 26.44 eV. This is due to being on the low energy side of the strong 2s – 2p absorption line. While not shown in the figure, as one continues to ionize Ne to doubly-ionized the strong 2s-2p line moves to lower energy at 25.33 eV and the net result is f_1 reaches a positive value of 3.9 at the 26.44 eV photon energy. In a real experiment using the Ar X-ray laser one could observe the neutral Ne gas go from opaque to transparent as the gas is ionized and furthermore watch the fringe shifts go from negative to positive as Ne is ionized from singly to doubly ionized. At some point there would be no fringe shift when there was the right mixture of singly and doubly ionized Ne. One could even envision using the ionization state of Ne as a switch that could move the Ar X-ray laser from one direction to another.

For Na we have a slightly simpler situation. Neutral Na has its L-edge at 30.6 eV and this moves to higher energy as Na is ionized so Na starts out quite transparent to the Ar X-ray laser photons at 26.44 eV. Fig. 3 shows the absorption constant f_2 versus photon energy for the two cases with Z* = 0 (Henke data) and Z* = 2.0 (average atom code with temperature of 7.3 eV). The doubly ionized case has the spectrum shifted by 5.5 eV so that the 2s-2p line agrees with the experimentally measured value of 32.7 eV [25]. If we now plot the optical constant f_1 versus photon energy for the two cases above, as show in Fig. 4, f_1 = -0.87 for neutral Na and goes to 1.44 for doubly-ionized Na. For singly ionized case the average atom code estimates a value of –0.15 for f_1. This suggests that an experiment with neutral Na gas would observe the anomalous dispersion and the fringe shifts would go through a zero point near singly ionized Na and eventually look quite normal as one approached doubly-ionized Na. Keep in mind that f_1 is still not equal to Z* for doubly-ionized Na so the measured electron density in an actual experiment would still be low by the ratio of f_1 to Z*.
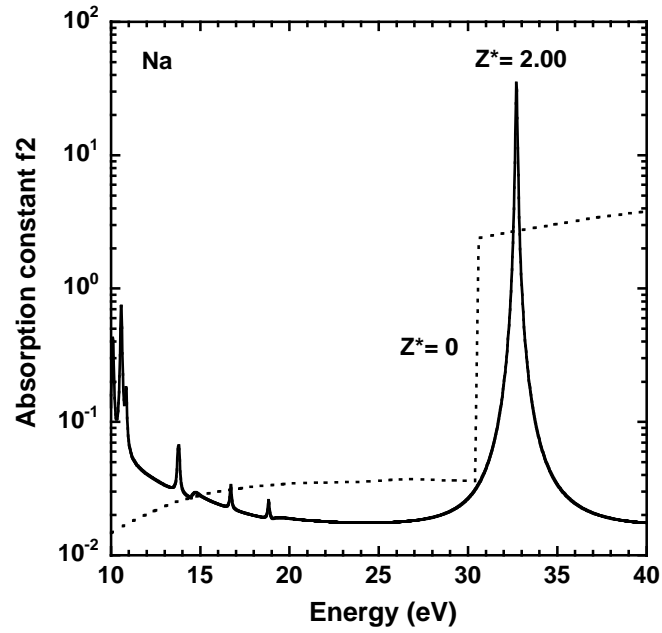
Fig. 3. Absorption constant f_2 versus photon energy for Na plasmas. The dotted line is from the Henke data. The solid curve is from the average atom code for $Z^* = 2.0$. The average ionization state is given by Z^*. The ion density is 10^{20} cm^{-3}.
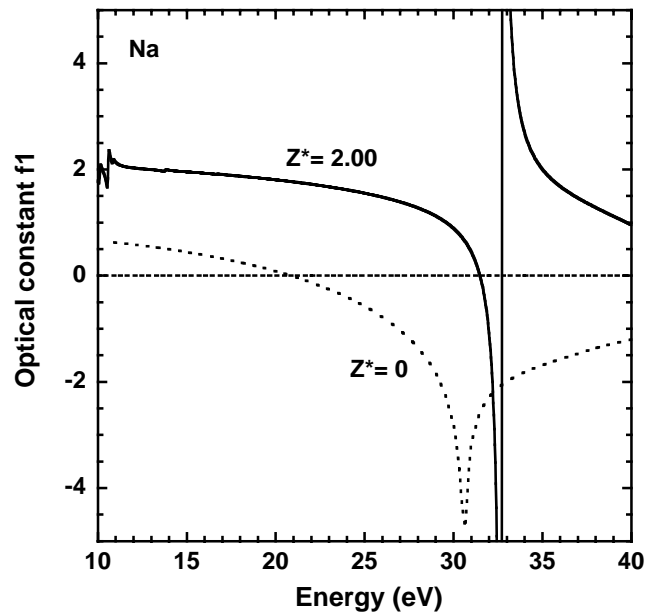

Fig. 4. Optical constant f_1 versus photon energy for Na plasmas. The dotted line is from the Henke data. The solid curve is from the average atom code for $Z^* = 2.0$. The average ionization state is given by Z^*. The ion density is 10^{20} cm^{-3}. The other dotted line at a value of 0 is a visual aid.
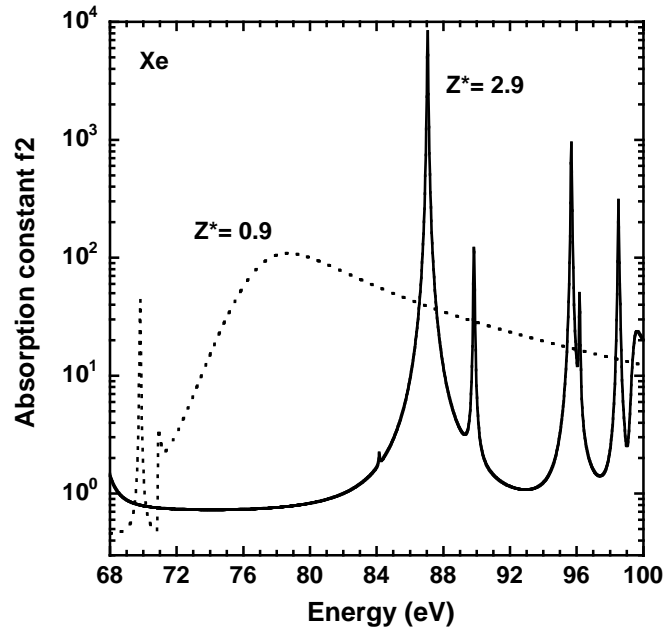
Fig. 5. Absorption constant f_2 versus photon energy for Xe plasmas. The average ionization state is given by Z*. The dotted line is for Z* = 0.9 and the solid curve is for Z* = 2.9. The ion density is 10^{20} cm^{-3}.
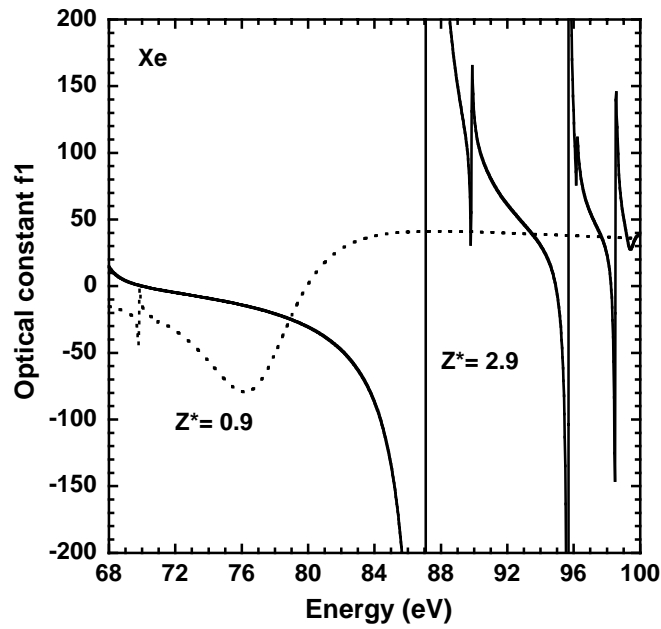

Fig. 6. Optical constant f_1 versus photon energy for Xe plasmas. The average ionization state is given by Z*. The dotted line is for Z* = 0.9 and the solid curve is for Z* = 2.9. The ion density is 10^{20} cm^{-3}.

5. MODELING OF XENON PLASMAS AT 14.7 NM

The Henke tables show neutral Xe with a value of –9 for f_1 at 14.7 nm (84.46 eV), the energy of the Ni-like Pd X-ray laser. We have recently improved the average atom code so we can do calculations of materials like Xe. Xe is an interesting case because the oscillator strength for the 4d state is primarily spread among the continuum photo-ionizations for neutral Xe through Xe^{2+} but suddenly collapses into the 4d – 4f transition as the 4f orbital becomes bound for Xe^{3+}. Figure 5 shows the absorption constant f_2 calculated by the average atom code for the cases of Xe with $Z^* = 0.9$ and $Z^* = 2.9$. The spectra are shifted by 2.5 and 8.5 eV, respectively, to agree better with the experimental data for Xe^{1+} and Xe^{3+}. One observes how the absorption goes from being spread over 10's of eV for the singly-ionized case ($Z^*=0.9$) to being largely concentrated in the single 4d – 4f line at 87 eV for the triply ionized case ($Z^*=2.9$). In both cases the total oscillator strength associated with the 4d level is about 10. If we now look at the optical constant f_1, Fig. 6 shows how f_1 is a large negative value below the 87 eV line for the case of $Z^* = 2.9$ while for the $Z^*=0.9$ case f_1 is positive and the plasma is highly absorbing. Recently Erik Emmons and his colleagues did a excellent set of experiments [26] at the Advance Light Source (ALS) at Lawrence Berkeley Laboratory to measure the absorption coefficient of Xe^{+3} with high resolution (0.05 eV) over the 37 to 117 eV region. Emmons graciously provided us with their detailed data so that we could calculated the optical constant f_1 from the absorption spectrum for Xe^{3+}. This is shown in Fig. 7. At 84.46 eV, f_1 is –35, which means there should be a tremendous negative fringe shift with the index of refraction larger than one. From 72 to 87 eV f_1 is negative. This is primarily due to the very strong 4d – 4f line at 87.0 eV. For the Ni-like Ag X-ray laser that lases at 13.9 nm (89.25 eV) f_1 is 16 since the laser line is on the high-energy side of the Xe^{+3} absorption line. In this case the experiment would bend the normal direction but the experiment would overestimate the electron density by a factor of five. Fig. 7 helps validate our calculations shown in Fig. 6.
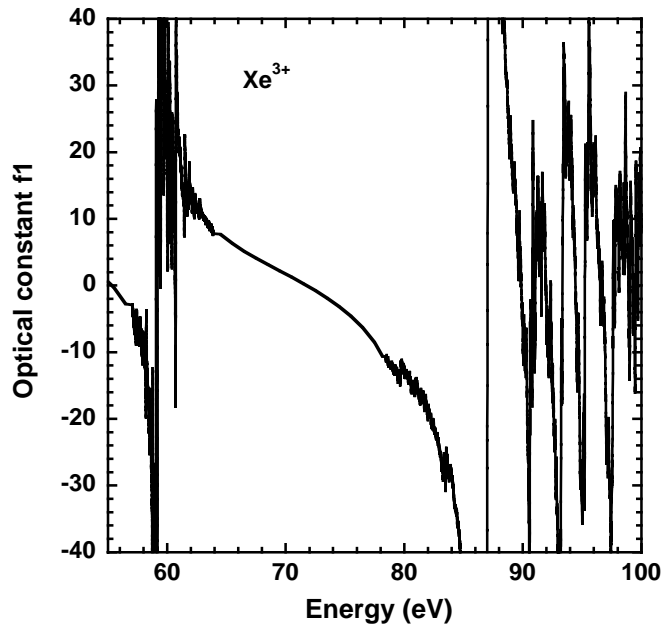

Fig. 7. Optical constant f_1 versus photon energy for Xe^{3+} calculated from experimental data in Ref. 26.

6.   CONCLUSIONS

Since the earliest days of lasers the analysis of plasma diagnostics such as interferometers have relied on the approximation that the index of refraction in plasmas is due solely to the free electrons. This makes the index of refraction less than one and is an essential assumption used in determining the critical density surface for energy deposition in the plasma and for doing photon transport calculations. Recent X-ray laser interferometer measurements of C, Al, Ag, and Sn plasmas have observed anomalous results with the index of refraction being greater than one. The analysis of these plasmas show that the anomalous dispersion from both the resonance lines and absorption edges due to the bound electrons can have the dominant contribution to the index of refraction. It is well known that a strong resonance line can cause anomalous results near the absorption line but this work shows that the effects from the resonance lines extend to photon energies located orders of magnitude further from the line centers than the corresponding line widths owing to the fact that they contribute through a dispersion integral. Similar long-range effects are shown for the absorption edges.

In this paper we search for other candidate materials that would have an index of refraction greater than one. Utilizing our average atom code we calculate the index of refraction in Ne, Na, and Xe plasmas, which we identified as candidate materials that would have anomalous dispersion for photon energies from the optical to 100 eV soft X-rays. We show that singly-ionized neon and neutral sodium should have an index greater than one at the energy of the Ne-like Ar X-ray laser at 46.9 nm (26.44 eV). We also show that triply-ionized xenon looks like a promising candidate at the 84.46 eV energy of the interferometer based on the Ni-like Pd X-ray laser. Finally we use recent high-resolution absorption measurements of triply-ionized xenon done at the ALS to validate our average atom calculations for Xe.

With the advent of the FLASH X-ray free electron laser in Germany and the LCLS X-FEL coming online at Stanford in 2 years the average atom code will be an invaluable tool to explore plasmas at higher X-ray energy to identify potential experiments for the future. During the next decade X-ray free electron lasers and other sources will be available to probe a wider variety of plasmas at higher densities and shorter wavelengths so it will be even more essential to understand the index of refraction in plasmas. X-ray laser interferometers may become a valuable tool to measure the index of refraction of plasmas in the future.

ACKNOWLEDGEMENTS

REFERENCES

[1] G. J. Tallents, J. Phys. D. **17**, 721 (1984).

[2] H. R. Griem, *Principles of Plasma Spectroscopy*, (Cambridge University Press, Cambridge, 1997) p. 9

[3] L. B. Da Silva, T. W. Barbee, Jr., R. Cauble, P. Celliers, D. Ciarlo, S. Libby, R. A. London, D. Matthews, S. Mrowka, J. C. Moreno, D. Ress, J. E. Trebes, A. S. Wan, and F. Weber, Phys. Rev. Lett. **74**, 3991 (1995).

[4] H. Tang, O. Guilbaud, G. Jamelot, D. Ros, A. Klisnick, D. Joyeux, D. Phalippou, M. Kado, M. Nishikino, M. Kishimoto, K. Sukegawa, M. Ishino, K. Nagashima, and H. Daido, Appl. Phys. B **78**, 975 (2004).

[5] J. Filevich, J. J. Rocca, M. C. Marconi, S. Moon, J. Nilsen, J. H. Scofield, J. Dunn, R. F. Smith, R. Keenan, J. R. Hunter, and V. N. Shlyaptsev, Phys. Rev. Lett. **94**, 035005 (2005).

[6] J. Filevich, K. Kanizay, M. C. Marconi, J. L. A. Chilla, and J. J. Rocca, Opt. Lett **25**, 356 (2000).

[7] D. Descamps, C. Lyngå, J. Norin, A. L'Hullier, C.-G. Wahlström, J.-F. Hergott, H. Merdji, P. Salières, M. Bellini, and T. W. Hänsch, Opt. Lett. **25**, 135 (2000).

[8] A. Meseck, M. Abo-Bakr, D. Krämer, B. Kuske, and S. Reiche, Nucl. Inst. And Meth. A **528**, 577 (2004).

[9] J. Filevich, J. J. Rocca, M. C. Marconi, S. J. Moon, J. Nilsen, J. H. Scofield, J. Dunn, R. F. Smith, R. Keenan, J. R. Hunter, and V. N. Shlyaptsev, J. Quant. Spectrosc. Radiat. Transfer **99**, 165 (2006).

[10] J. Filevich, J. Grava, M. Purvis, M. C. Marconi, J. J. Rocca, J. Nilsen, J. Dunn, W. R. Johnson, Phys. Rev. E 74, 016404 (2006).

[11] J. Filevich, J. Grava, M. Purvis, M. C. Marconi, J. J. Rocca, J. Nilsen, J. Dunn, W. R. Johnson, Laser and Particle Beams **25**, 47 (2007).

[12] J. Nilsen and J. H. Scofield, Opt. Lett. **29**, 2677 (2004).

[13] J. Nilsen, W. R. Johnson, C. A. Iglesias, and J. H. Scofield, J. Quant. Spectrosc. Radiat. Transfer **99**, 425 (2006).

[14] J. Nilsen and W. R. Johnson, Appl. Opt. **44**, 7295 (2005).

[15] D. A. Liberman, JQSRT **27**, 335 (1982).

[16] W. R. Johnson, C. Guet, and G. F. Bertsch, J. Quant. Spectrosc. Radiat. Transfer **99**, 327 (2006).

[17] C. A. Iglesias, F. J. Rogers, and B. G. Wilson, Astrophys. J. Lett. **322**, L45 (1987).

[18] F. J. Rogers, B. G. Wilson, and C. A. Iglesias, Phys. Rev. A **38**, 5007 (1988).

[19] C. A. Iglesias and F. J. Rogers Astrophys. J. **464**, 943 (1996).

[20] B. L. Henke, E. M. Gullikson, and J. C. Davis, ADNDT **54**, 181 - 342 (1993).

[21] L. D. Landau and E. M. Lifshitz, *Electrodynamics of Continuous Media*, (Pergamon, New York, 1984) pp. 280 - 283

[22] D. A. Greenwood, Proc. Phys. Soc. London **715**, 585 (1958).

[23] R. Kubo, J. Phys. Soc. Jpn. **12**, 570 (1957).

[24] W. Persson, Phys. Scr. 3, 133 (1971).

[25] T. Lundstrom and L. Minnhagen, Phys. Scr. 5, 243 (1972).

[26] E. D. Emmons, A. Aguilar, M. F. Gharaibeh, S. W. J. Scully, R. A. Phaneuf, A. L. D. Kilcoyne, A. S. Schlachter, I. Àlverez, C. Cisneros, and G. Hinojosa, Phys. Rev. A **71**, 042704 (2005).